[10] R. G. Harrison, "Theory of regenerative frequency dividers using double-balanced mixers," in *1989 IEEE MTT-S. Int. Microwave Symp. Dig.*, pp. 459–462.
[11] R. Ranfft and H.-M. Rein, "A simple but efficient analog computer for simulation of high-speed integrated circuits," *IEEE J. Solid-State Circuits*, vol. SC-12, pp. 51–58, Feb. 1977.
[12] V. Lück, "Untersuchungen an einem regenerativen Frequenzteiler für den GHz-Bereich," Diploma thesis, Inst. of Electronics of Ruhr-University Bochum, Arbeitsgruppe Halbleiterbauelemente, Bochum, F. R. Germany, 1985.
[13] G. Hüther, "Dynamische Teiler für Anwendungen in der digitalen Gigabit/s-Technik," Diploma thesis, Inst. of Technical Electronics of the Technical University of Aachen, Aachen, F. R. Germany, 1988.
[14] H.-M. Rein, "Dynamischer Frequenzteiler mit Mischstufe und Verstärker," G. German patent P 3509 327, 1987.

A Multistrip Moment Method Technique and Its Application to the Post Problem in a Circular Waveguide

Xiao-Hui Zhu, Dai-Zong Chen, and Shi-Jin Wang

Abstract—**A moment method technique for solving obstacle problems in a waveguide is presented. Instead of the procedure using a multifilament current representation, which leads to a slowly converging series, a multistrip representation of the current is proposed. In the procedure, the true currents on obstacle surfaces are replaced by equivalent planar currents in a number of waveguide cross sections inside the obstacle. The technique is applied to a pair of metallic posts in the TE_{11}-mode circular waveguide. Numerical results are compared with experimental data.**

I. Introduction

The moment method (MM) is one of the most efficient numerical methods and has been widely used for solving such waveguide problems as discontinuities, junctions, transitions, excitations, obstacles, and eigenvalue problems [1]–[9]. For the inductive post in a rectangular waveguide, a two-dimensional MM solution was developed by Leviatan *et al.* [5], [6], who computed the parameters of the equivalent circuit and current distribution for a post of large diameter. For the probe-excited rectangular waveguide, a three-dimensional MM solution was developed by Jarem [7], who gave the input impedance and surface currents on the probe. These MM solutions used a multifilament current representation for the post, or probe; we refer to these as multifilament MM's. In the multifilament MM procedure, the true electric currents induced on the obstacle surfaces are replaced by a number of filamentary currents inside the obstacles. The boundary condition is then tested on the obstacle surfaces and a set of linear equations, i.e., a matrix equation, is derived. A shortcoming of the multifilament MM is that the value of matrix elements tends to infinity as the electric-field testing point approaches the filament. If the Green's function is expressed as an infinite summation of normal mode functions which satisfy the boundary condition on the waveguide wall, the matrix elements will be led to a slowly converging series, which is not convenient for computation. In a rectangular waveguide, fortunately, this series can be converted to a rapidly converging one by introducing an auxiliary series [5]–[7], or the static Green's function [2], and the multifilament MM can then be used successfully for the post and probe problems. In waveguides having other cross sections, to the authors' knowledge, such an auxiliary series is difficult to find. As a result, the multifilament MM has only a restricted application.

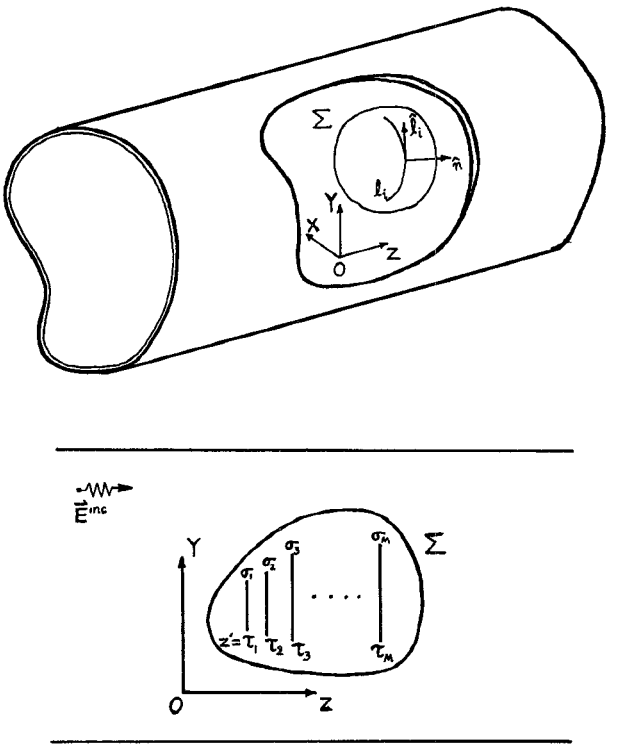

Fig. 1. Obstacle and imaginary strips in a waveguide.

In this paper, a multistrip current representation is introduced to develop a moment method technique for obstacle problems in waveguides of arbitrary section. The true currents on the obstacle surfaces are replaced by equivalent planar currents in a number of waveguide cross sections inside the obstacle, and the unknown planar currents are then expanded. The matrix equation is obtained by testing the tangential electric fields along properly chosen matching lines on the obstacle surfaces. The multistrip MM procedure will be described formally in Section II.

In a circular waveguide, the concentric discontinuities have been studied by many authors [8], [9]. By contrast, there has been little study of nonaxisymmetric discontinuities of circular waveguides, especially those with finite thickness. The multistrip MM should prove useful in solving such problems. The case of a pair of posts in a TE_{11}-mode circular waveguide will be analyzed in Section III.

II. Basic Formulation

The problem considered is depicted in Fig. 1. An obstacle is located in a cylindrical waveguide of arbitrary cross section whose axis is in the z direction. Extending the procedure to a

Manuscript received September 13, 1990; revised May 2, 1991.
The authors are with the Beijing Institute of Radio Measurement, Beijing 100039, People's Republic of China.
IEEE Log Number 9102329.

multiobstacle case is straightforward. The total fields, $\vec{E}$ and $\vec{H}$, are composed of incident and scattered fields:

$$\vec{E} = \vec{E}^{\text{inc}} + \vec{E}^{s} \tag{1a}$$

$$\vec{H} = \vec{H}^{\text{inc}} + \vec{H}^{s}. \tag{1b}$$

The obstacle is assumed to be perfectly conducting, so that the tangential components of the total electric field must vanish on the surface, Σ, while the tangential components of the total magnetic field are related to the surface current, $\vec{J}^{\Sigma}$, i.e.,

$$\hat{n} \times \vec{E} = 0 \qquad \text{on } \Sigma \tag{2a}$$

$$\vec{J}^{\Sigma} = \hat{n} \times \vec{H} \qquad \text{on } \Sigma \tag{2b}$$

where $\hat{n}$ is the outward normal to the surface. In order to find the scattered field in the waveguide, we replace the perfectly conducting obstacle surface, Σ, by an equivalent current distribution, $\vec{J}$, on M suitably chosen strips which are perpendicular to the waveguide axis, inside the obstacle. The current distribution, $\vec{J}$, is composed of a set of equivalent transverse currents, $\vec{J}_m$, $m = 1,2,\cdots,M$, carried by strip σ_m on the plane $z' = \tau_m$, as shown in Fig. 1. The scattered field is then expressed by

$$\vec{E}^{s} = \sum_{m=1}^{M} \int_{\sigma_m} \overline{\overline{G}}_t(x,y,z|x',y',z') \cdot \vec{J}_m(x',y')\, d\sigma_m \tag{3}$$

where the dyadic Green's function, $\overline{\overline{G}}_t$, is defined as the electric field radiated by a unit transverse current source at (x', y', z') in the waveguide with the obstacle removed, i.e.,

$$\nabla \times \nabla \times \overline{\overline{G}}_t - k^2 \overline{\overline{G}}_t = -j\omega\mu\left(\hat{x}\hat{x} + \hat{y}\hat{y}\right)\delta(x-x')\delta(y-y') \tag{4}$$

where $k = 2\pi/\lambda = \omega(\mu\epsilon)^{1/2}$, and λ is the free-space wavelength. By using the Lorentz reciprocity principle, the dyadic Green's function can be expressed in terms of waveguide modes as follows [10]:

$$\overline{\overline{G}}_t = -\frac{1}{2}\sum_p \vec{E}_p^{\pm}(x,y,z)\vec{e}_p(x',y')e^{\mp\nu_p z'} \qquad \begin{matrix} z > z' \\ z < z' \end{matrix} \tag{5}$$

where the fields for the pth mode propagating (or evanescing) in the $+z$ direction, $\vec{E}_p^{+}$ and $\vec{H}_p^{+}$, and those in the $-z$ direction, $\vec{E}_p^{-}$ and $\vec{H}_p^{-}$, are represented by

$$\vec{E}_p^{\pm} = \left(\vec{e}_p \pm e_{pz}\hat{z}\right)e^{\mp\nu_p z} \tag{6a}$$

$$\vec{H}_p^{\pm} = \left(\pm\vec{h}_p + h_{pz}\hat{z}\right)e^{\mp\nu_p z}. \tag{6b}$$

In (6), $\vec{e}_p$ and $\vec{h}_p$ are orthogonal transverse vector functions and have been normalized in the form

$$\iint_A \vec{e}_p \times \vec{h}_{p'} \cdot \hat{z}\, dA = \delta_{pp'} \tag{7}$$

where A is the waveguide cross section and $\delta_{pp'}$ is the Kronecker delta. Generally, the sum in (5) includes all TE_{nq} and TM_{nq} modes. Substitution of (6) into (5) gives

$$\overline{\overline{G}}_t = -\frac{1}{2}\sum_p \left[\vec{e}_p(x,y) \pm e_{pz}(x,y)\hat{z}\right] \cdot \vec{e}_p(x',y')e^{-\nu_p|z-z'|} \qquad \begin{matrix} z > z' \\ z < z' \end{matrix}. \tag{8}$$

The current, $\vec{J}_m$, in (3) is expressed in terms of expansion functions, f_j, as follows:

$$\vec{J}_m = \sum_{j=s_{m-1}+1}^{s_m} I_j f_j(x',y')\hat{t}_j \qquad \text{on } \sigma_m$$

$$z' = \tau_m \qquad m = 1,2,\cdots,M \qquad s_0 = 0$$

where $\hat{t}_j$ is a unit transverse vector. I_j, $j = 1,2,\cdots,s_M$, is a constant yet to be determined. On the obstacle surface, Σ, a finite number of matching lines, l_t, are chosen to test the boundary conditions (see Fig. 1). For each line, a number of weighting functions, w_i, may be used. That is,

$$\int_{l_t} w_t \hat{l}_t \cdot \vec{E}\, dl = 0, \qquad i = 1,2,\cdots,K \tag{9}$$

where $\hat{l}_t$ is a unit tangential vector of surface Σ along line l_t. As a result, a system of linear equations, i.e., a matrix equation, is obtained:

$$\boldsymbol{ZI} = \boldsymbol{V} \tag{10}$$

where

$$Z_{tj} = \frac{1}{2}\sum_p L_{p,j}e^{-\nu_p|z_t - z_j'|}\int_{l_t} w_t\left(\vec{e}_p \pm e_{pz}\hat{z}\right)\cdot\hat{l}_t\, dl \qquad \begin{matrix} z_t > z_j' \\ z_t < z_j' \end{matrix} \tag{11}$$

$$L_{p,j} = \int_{\sigma_m} f_j \vec{e}_p \cdot \hat{t}_j\, d\sigma \tag{12}$$

$$V_t = \int_{l_t} w_t \vec{E}^{\text{inc}} \cdot \hat{l}_t\, dl. \tag{13}$$

Generally, the number of equations in system (10) is taken to be equal to the total number of unknowns, and the solution of (10) is straightforward. Once (10) is solved, the scattered fields from the obstacle are then obtained as

$$\vec{E}^{s}(x,y,z) = \sum_p b_p^{+}\vec{E}_p^{+} + \sum_p b_p^{-}\vec{E}_p^{-} \tag{14a}$$

$$\vec{H}^{s}(x,y,z) = \sum_p b_p^{+}\vec{H}_p^{+} + \sum_p b_p^{-}\vec{H}_p^{-} \tag{14b}$$

where

$$b_p^{+} = \sum_{z_j' < z} I_j L_{p,j} e^{\nu_p z_j'} \tag{15a}$$

$$b_p^{-} = \sum_{z_j' > z} I_j L_{p,j} e^{-\nu_p z_j'}. \tag{15b}$$

The values of b_p^{+} and b_p^{-} vary with z in the range $\tau_1 < z < \tau_M$, while $b_p^{+} = 0$ for $z < \tau_1$, and $b_p^{-} = 0$ for $z > \tau_M$.

III. Posts in Circular Waveguide

The multistrip MM procedure presented here has been used to analyze a pair of posts in a circular waveguide, as shown in Fig. 2 [11]. The geometry and coordinate system are illustrated in Fig. 3. It is assumed that only the TE_{11} mode, $p = 1$, can propagate in the waveguide, so that

$$0.2930 < a/\lambda < 0.3827 \tag{17}$$

where a is the waveguide radius. Consider the case of two strips and a four-term expansion, i.e.,

$$M = 2 \qquad \tau_1 = -c \qquad \tau_2 = c \qquad s_1 = 4 \qquad s_2 = 8.$$

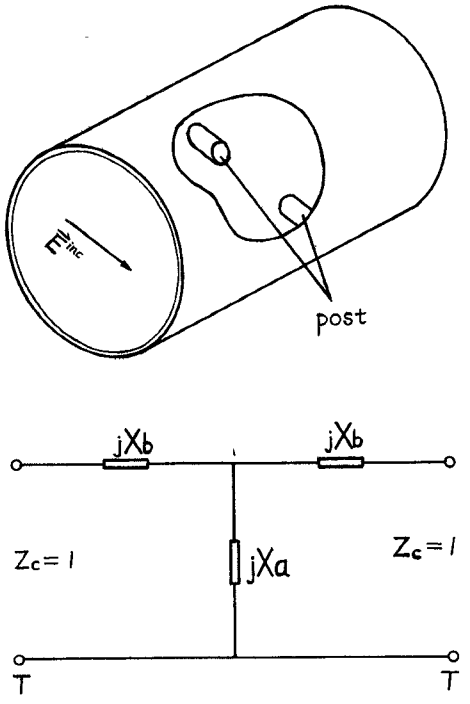

Fig. 2. A pair of posts in circular waveguide and their equivalent circuit.

In view of the fact that both the posts and incident electric field are x-directed, the equivalent currents can be expressed as

$$\vec{J}_1 = \hat{x} \sum_{j=1}^{4} I_j f_j(x', y') \qquad \text{on } \sigma_1,\ z_j' = -c \tag{18a}$$

$$\vec{J}_2 = \hat{x} \sum_{j=5}^{8} I_j f_j(x', y') \qquad \text{on } \sigma_2,\ z_j' = c \tag{18b}$$

where

$$f_j(x, y) = \psi_j(x)\zeta_j(y) \tag{19}$$

$$\psi_1 = \psi_3 = \psi_5 = \psi_7 \qquad \psi_2 = \psi_4 = \psi_6 = \psi_8 \tag{20}$$

$$\zeta_1 = \zeta_2 = \zeta_5 = \zeta_6 \qquad \zeta_3 = \zeta_4 = \zeta_7 = \zeta_8 \tag{21}$$

$$\psi_1(x) = \sin ku \tag{22a}$$

$$\psi_2(x) = \alpha(1 - \cos ku) - \sin ku \tag{22b}$$

$$\alpha = \frac{kh - \sin kh \cos kh}{(1 - \cos kh)^2}$$

$$u = x - a + h$$

$$\zeta_1(y) = \frac{1}{b} \tag{23a}$$

$$\zeta_3(y) = \frac{\pi}{2b} \cos \frac{\pi y}{b} - \frac{1}{b} \tag{23b}$$

with h the post length and b the strip width. The constant α makes ψ_1 and ψ_2 orthogonal to one another in the interval $0 < u < h$ [7]. The strips σ_1 and σ_2 must be within the post of diameter d; hence

$$0 < c < d/2 \tag{24}$$

$$0 < b \leqslant (d^2 - 4c^2)^{1/2}. \tag{25}$$

It is convenient to select six generatrix lines equally spaced on the post surface as matching lines. Symmetry shows that only four lines (denoted *1*, *2*, *3*, and *4* in Fig. 3) need to be tested. The $\psi_1(x)$ and $\psi_2(x)$ of (22) are used as the weighting functions for each matching line. From (20) we have

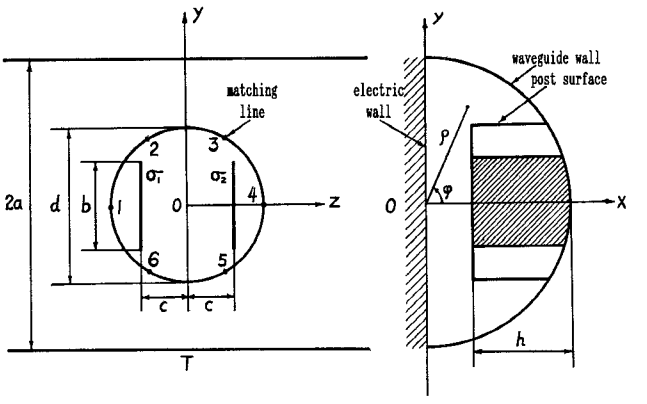

Fig. 3. Multistrip current representation.

$$w_i = \psi_i(x) \qquad \hat{l}_i = \hat{x}, \qquad i = 1, 2, \cdots, 8.$$

Therefore (11)–(13) become

$$z_{ij} = \frac{1}{2} \sum_p L_{p,j} e^{-\nu_p |z_i - z_j'|} \int_0^{H(y_i)} \psi_i(x) e_{px}(x, y_i)\, du \tag{26}$$

$$L_{p,j} = 2 \int_{-b/2}^{b/2} \int_0^{H(y')} e_{px}(x', y') f_j(x', y')\, du'\, dy' \tag{27}$$

$$V_i = e^{-j\beta_1 z_i} \int_0^{H(y_i)} \psi_i(x) e_{1x}(x, y_i)\, du \tag{28}$$

where

$$H(y) = h - a + (a^2 - y^2)^{1/2} \tag{29}$$

is the length of matching line or strip in the x direction, and $\beta_1 = \nu_1 / j$ is the propagation constant of the dominant mode TE_{11}. In the structure considered, only the modes with $\cos n\phi$ variations in $e_{p\rho}$ can be excited and e_{px} in (26)–(28), for the TE_{nq} mode, is expressed by

$$e_{px} = \sqrt{K'_{nq}}\, C'_{nq} \left[J_n\left(\mu'_{nq} \frac{\rho}{a}\right) \frac{nx}{\mu'_{nq} \rho^2} \cos n\phi + J'_n\left(\mu'_{nq} \frac{\rho}{a}\right) \frac{y}{a\rho} \sin n\phi \right] \tag{30}$$

where

$$K'_{nq} = \sqrt{\frac{\mu}{\epsilon}}\, \frac{jk}{\nu_p}$$

$$C'_{nq} = \sqrt{\frac{2}{\pi(1 + \delta_{n0})}}\, \frac{\mu'_{nq}}{\sqrt{\mu'^2_{nq} - n^2} J_n(\mu'_{nq})}$$

$$\nu_p = k \sqrt{\left(\frac{\mu'_{nq}}{2\pi} \frac{\lambda}{a}\right)^2 - 1}\,.$$

For the TM_{nq} mode,

$$e_{px}=\sqrt{K_{nq}}\,C_{nq}\left[J_n'\left(\mu_{nq}\frac{\rho}{a}\right)\frac{\mu_{nq}x}{a\rho}\cos n\phi+J_n\left(\mu_{nq}\frac{\rho}{a}\right)\frac{ny}{\rho^2}\sin n\phi\right] \tag{31}$$

where

$$K_{nq}=\sqrt{\frac{\mu}{\epsilon}}\,\frac{\nu_p}{jk}$$

$$C_{nq}=\sqrt{\frac{2}{\pi(1+\delta_{n0})}}\,\frac{1}{\mu_{nq}J_n'(\mu_{nq})}$$

$$\nu_p=k\sqrt{\left(\frac{\mu_{nq}}{2\pi}\frac{\lambda}{a}\right)^2-1}\,.$$

Here $J_n(x)$ is the Bessel function, and μ_{nq} and μ'_{nq} are the qth roots of $J_n(x)=0$ and $J_n'(x)\equiv dJ_n(x)/dx=0$, respectively. In the summation (26), only the TE_{nq} and TM_{nq} modes with odd index n are needed because the $x=0$ plane is an electric wall.

The reflection and transmission coefficients for the incident TE_{11} mode or the scattering-matrix parameters for the equivalent circuit are then obtained as

$$S_{11}=S_{22}=b_1^-$$

$$S_{12}=S_{21}=1+b_1^+$$

where $b_1^{\mp}$ can be derived from (15), in which the observation points were taken to be far away from the posts, i.e., $z\ll\tau_1=-c$ or $z\gg\tau_2=c$. This is true even though the reference plane T of the equivalent circuit in Fig. 2 is taken as the central plane of $z=0$ (Fig. 3). It then follows that

$$b_1^{\pm}=\sum_{j=1}^{4}I_jL_{1,j}e^{\mp j\beta_1 c}+\sum_{j=5}^{8}I_jL_{1,j}e^{\pm j\beta_1 c}. \tag{32}$$

The parameters of the equivalent circuit can be obtained by [5]

$$jX_a=\frac{2S_{12}}{(1-S_{11})^2-S_{12}^2} \tag{33a}$$

$$jX_b=\frac{1+S_{11}-S_{12}}{1-S_{11}+S_{12}}. \tag{33b}$$

A computer program has been prepared to carry out the solution procedure. A 32-point Gaussian quadrature is used to evaluate the integral over the interval $0<u<H(y)$, which is divided into Nx segments:

$$Nx=1+\mathrm{Int}\left(0.7\frac{h}{a}q\right)+\mathrm{Int}\left(\frac{n}{13}\right).$$

Similarly, a three-point Gaussian quadrature is used for the integral over the interval $-b/2<y'<b/2$ with Ny segments:

$$Ny=1+\mathrm{Int}\left(n\frac{b}{a}\right).$$

In order to test the convergence of the multistrip MM procedure, the summation (26) over different higher order modes is computed for typical dimensional parameters ($0.02<d/\lambda<0.1, h/a<0.5$) in the frequency band of (17). It is found that TE_{n1}, TE_{n2}, TM_{n1}, TM_{n2}, and TM_{n3} make a significant contribution to z_{ij}. The contribution of TM_{nq} with $q>3$ is found to be small, and TE_{nq} with $q>2$ can be ignored. The equivalent circuit parameters are insensitive to the width, b, and location, c, of strips except for the values close to the limits of (24) and (25). The calculated values of normalized Xa and Xb for $a/\lambda=0.321$ and 0.355 were illustrated in [11].

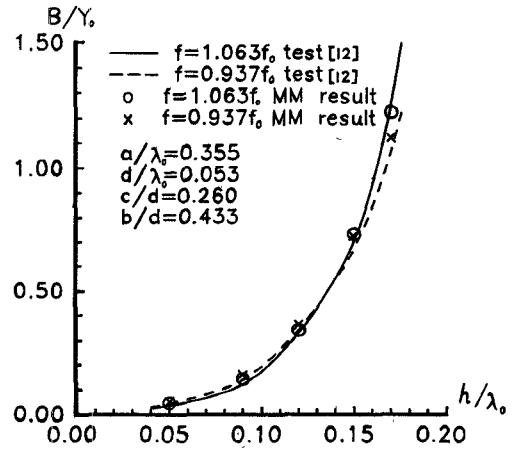

Fig. 4. Equivalent susceptance of posts.

A comparison between numerical results and measured data given by Ishida *et al.* [12] for the post normalized susceptance $B(=-1/X_a)$ is shown in Fig. 4.

IV. Conclusion

The multistrip moment method procedure for the analysis of a metal obstacle in a waveguide is formulated by introducing equivalent planar currents within the obstacle and matching lines on the obstacle surface. In this procedure, the matrix elements are determined by a series involving integrals of mode functions over the strips and the convergence has been improved. As an example, the technique is applied to a pair of posts in a circular waveguide. The computed results show good agreement with the experimental data.

References

[1] H. Auda and R. F. Harrington, "A moment solution for waveguide junction problems," *IEEE Trans. Microwave Theory Tech.*, vol. MTT-31, pp. 515–520, July 1983.

[2] H. Auda and R. F. Harrington, "Inductive posts and diaphragms of arbitrary shape and number in a rectangular waveguide," *IEEE Trans. Microwave Theory Tech.*, vol. MTT-32, pp. 606–613, June 1984.

[3] W. A. Huting and K. J. Webb, "Numerical solution of the continuous waveguide transition problem," *IEEE Trans. Microwave Theory Tech.*, vol. 37, pp. 1802–1808, Nov. 1989.

[4] A. S. Omar and K. F. Schunemann, "Analysis of waveguides with metal inserts," *IEEE Trans. Microwave Theory Tech.*, vol. 37, pp. 1924–1932, Dec. 1989.

[5] Y. Leviatan, P. G. Li, A. T. Adams, and J. Perini, "Single-post inductive obstacle in rectangular waveguide," *IEEE Trans. Microwave Theory Tech.*, vol. MTT-31, pp. 806–812, Oct. 1983.

[6] Y. Leviatan, D. H. Shau, and A. T. Adams, "Numerical study of the current distribution on a post in a rectangular waveguide," *IEEE Trans. Microwave Theory Tech.*, vol. MTT-32, pp. 1411–1415, Oct. 1984.

[7] J. M. Jarem, "A multifiliament method-of-moments solution for the input impedance of a probe-excited semi-infinite waveguide," *IEEE Trans. Microwave Theory Tech.*, vol. MTT-35, pp. 14–19, Jan. 1987.

[8] R. W. Scharstein and A. T. Adams, "Galerkin solution for the thin circular iris in a TE11-mode circular waveguide," *IEEE Trans. Microwave Theory Tech.*, vol. 36, pp. 106–113, Jan. 1988.

[9] R. W. Scharstein and A. T. Adams, "Thick circular iris in a TE11 mode circular waveguide," *IEEE Trans. Microwave Theory Tech.*, vol. 36, pp. 1529–1531, Nov. 1988.

[10] R. E. Collin, *Field Theory of Guided Waves*. New York: McGraw-Hill, 1960, pp. 198–209.
[11] X.-H. Zhu, D.-Z. Chen, and S.-J. Wang, "Method-of-moments solution for the posts in a circular waveguide," in *IEEE MTT-S Int. Microwave Symp. Dig.* (Dallas, TX), May 8–10, 1990, pp. 693–696.
[12] Q. Ishida, S. Kaniya, and F. Takde, "A design method of polarizer using metallic posts," *Tech. Rep. Inst. Electron. and Commun. Eng. Japan*, vol. 78, no. 178, MW78-83, pp. 1–6, Sept. 24, 1978.

Numerical Analysis of Waveguide Discontinuity Problems Using the Network Model Decomposition Method

Geyi Wen

Abstract—**This paper presents an application of the network model decomposition method to the analysis of arbitrarily shaped H- and E-plane waveguide junctions. By using the polygon discretization technique introduced in [1], the waveguide discontinuity region, which is surrounded by a metallic wall and the reference planes chosen, is first discretized; then the topological model and the corresponding network model for the waveguide discontinuity are established. In the formulation, equivalent current sources connected to the nodes on the boundary of the region have been introduced to replace the effect of the field external to the region. The field internal to the region is approximated by the nodal voltage distribution of the network model, which can then be used to determine the scattering parameters of the waveguide junction. A diakoptic algorithm for the solution of the network model has also been developed. To illustrate the applications and show the validity of the method, numerical results for various H- and E-plane junctions have been given and a favorable comparison has been made with other existing theories.**

I. Introduction

In an earlier paper, a method termed network model decomposition (NMD) was presented for the solution of transmission line problems. The object of the present paper is to describe the application of the NMD method to the analysis of scattering by H- or E-plane waveguide junctions. A topological model for the waveguide discontinuity is first established by dividing the discontinuity region into polygonal subregions; the corresponding network model is then formulated on the basis of the topological model and the field equations. In the formulation, the field internal to the waveguide discontinuity region is discretized and represented by a nodal voltage distribution. The field external to the region is replaced by equivalent current sources connected to the boundary nodes, without affecting the field distribution inside the region. A diakoptic algorithm is also developed for the solution of the network models, by means of which the computational efforts and computer core storage can be greatly reduced.

To show the validity and usefulness of the network model decomposition method, computed results are given for various H- and E-plane waveguide discontinuities. In all cases studied, the power conservation condition is satisfied to an accuracy of $\pm 10^{-5}$.

Manuscript received June 12, 1990; revised January 2, 1991.
The author is with the Institute of Applied Physics, University of Electronic Science and Technology of China, Chengdu 610054, People's Republic of China.
IEEE Log Number 9101020.

II. Topological Models and Network Models

An arbitrarily shaped n-port waveguide junction is shown in Fig. 1(a), where the reference planes Γ_p $(p=1,2,\cdots,n)$ and the metallic wall Γ_0 completely enclose the waveguide discontinuity region Ω; d_p is the width, a_p, or the height, b_p, of the waveguide p for the H- or E-plane junction. The waveguide p is assumed to be filled with dielectric of relative permittivity ϵ_{rp}.

If the excitation by the dominant TE_{10} mode is assumed, then the waveguide discontinuity can be described by the following equations [9]:

$$\nabla^2\varphi + \hat{K}^2\varphi = 0 \tag{1}$$

$$\hat{K}_0^2 = K_0^2\hat{\epsilon}, \tag{2}$$

$$K_0^2 = \omega^2\mu_0\epsilon_0 \tag{3}$$

$$\hat{\epsilon}_r = \begin{cases} \epsilon_r & (\text{for } H\text{-plane junction}) \\ \epsilon_r - (\pi/K_0 a)^2 & (\text{for } E\text{-plane junction}) \end{cases} \tag{4}$$

$$\varphi = \begin{cases} E_z & (\text{for } H\text{-plane junction}) \\ H_z & (\text{for } E\text{-plane junction}) \end{cases} \tag{5}$$

where E_z and H_z are the z components of electric and magnetic field respectively.

Following the procedure described in [1], the waveguide discontinuity region is first discretized by using polygon discretization techniques (Fig. 1(b)). Then the topological model for the waveguide discontinuity problem can be established (Fig. 1(c)). The set of all the oriented branches and the incidence matrix of the topological model will be denoted by $S_b=\{b_1,b_2,\cdots,b_b\}$ and $A=\{a_{ij}\}$ respectively. Then we have the equivalent form of Kirchhoff's voltage laws as follows:

$$U_b = A^T V \tag{6}$$

where $V=(\varphi_1,\varphi_2,\cdots,\varphi_N)^T$ is the node-to-datum voltage vector; φ_k is the value of φ at node n_k $(k=1,2,\cdots,N)$; and U_b is the branch voltage vector.

Making use of the approximation introduced in [1], the node equation for an interior node n_k can be expressed in terms of the incidence matrix A as

$$\sum_{i=1}^{e_k} a_{kl_i} Y_{k_i} u_{l_i} = \sum_{l=1}^{b} a_{kl} i_{bl} = 0 \tag{7}$$

where u_{l_i} is the branch voltage, i_{bl} the branch current and Y_{k_i} the branch admittances:

$$\begin{cases} Y_{k_0} = -\hat{K}^2 S_k \\ Y_{k_i} = \left(\overline{p_{i-1}q_i} + \overline{q_i p_i}\right) \Big/ \overline{m_i n_k} \end{cases}. \tag{8}$$

We now construct the node equation for a boundary node. The dual element G_k of a boundary node n_k is shown in [1, fig. 2(b)]. The following relation can then be derived in a similar way:

$$\begin{aligned} &\sum_{i=2}^{e_k-1} \int_{\overline{p_{i-1}q_i p_i}} \frac{\partial\varphi}{\partial n}\, d\Gamma \\ &\quad + \int_{\overline{q_1 p_1}} \frac{\partial\varphi}{\partial n}\, d\Gamma + \int_{\overline{p_{e_k-1}q_{e_k}}} \frac{\partial\varphi}{\partial n}\, d\Gamma + \hat{K}^2 \iint_{G_k} \varphi\, ds \\ &\quad + \int_{\overline{n_k q_1}} \frac{\partial\varphi}{\partial n}\, d\Gamma + \int_{\overline{n_k q_{e_k}}} \frac{\partial\varphi}{\partial n}\, d\Gamma = 0. \end{aligned} \tag{9}$$